Journal of Applied Mechanics Vol. 3, pp. 481-488 (August 2000) JSCE

DISCONTINUOUS DEFORMATION ANALYSIS OF A SAND MODEL AND ITS MICROSCOPIC CONSIDERATION

不連続変形法による砂モデルの解析と微視的な検討

Guoxin Zhang*, Guangxin Li**, Yasuhito Sugiura* and Hiroo. Hasegawa*
張 国新・李 広信・杉浦 靖人・長谷川 浩夫
*INA Corporation. (1-44-10 Sekiguchi Bunkyo-ku, Tokyo)
**Professor of Tsinghua University of China. (Beijing 100084, China)

ABSTRACT: DDA (Discontinuous Deformation Analysis), a numerical method used to analyze the discontinuous media, is used to simulate the deformation mechanism of a sand model in this paper. The microscopic mechanism of deformation properties of a sand model such as elasto-plastisity, dilatancy, strain softening, hysteresis loop during unloading-reloading, volume contraction during unloading and formation of shear zone are analyzed and explained by the DDA simulation. The method that takes sand as discontinuous particles provides a powerful approach in the field of soil mechanics.

Key words: DDA, sand model, granular media, stress-strain relationship.

1. INTRODUCTION

It is well recognized that the stress-strain relationship of sand, such as elasto-plasticity, dilatancy, strain-softening, hysteresis loop during unloading-reloading and volume contraction during unloading, is very complicated. The mechanism of these phenomena has not been fully understood. Some explanations of the mechanism are given based on conjecture. Still there remain many aspects that puzzle the researchers of soil mechanics.

The complexity of the phenomena lies mainly on the discontinuity of sand. In fact, sand is composed particles of many kinds of mineral materials and is of air-liquid-solid three-phase in some cases. In numerical simulation, sand is usually treated as continuous media. Although it has been realized that the way of revealing the unique stress-strain relationship of sand through its microscopic aspects should be followed, it is too difficult to build quantitative relationship between microscopic and macroscopic behaviors. Hence the research on sand by using discontinuous media mechanism through its microscopic aspects mainly depended on perceptual understanding, qualitative analysis and theoretical analysis of particle movement. Rowe[1] studied the dilatancy property of soil by analyzing the movement pattern of particles under different stress condition. Some meaningful results were obtained. But a few assumptions were made in the study and an incorrect conclusion that dilatancy is unrecoverable was yielded.

Numerical simulation of particles is a useful way to reveal the deformation properties of sand from microscopic to macroscopic scale. There are a few methods can be selected, DEM (Distinct Element Method) and DDA (Discontinuous Deformation Method) are two of them.

DEM proposed by Cundall[2] takes every particle as an rigid isolated element. By analyzing the external force, contact force with the other particles and the inertia force acted on every particle, its motion can be calculated according to the Newton's second law of motion. Because there are no matrix equations needed to be solved, this method is very fast in solving the motion problem of granular assembly. But for

static and quasi-static problem, it will cause problems because the elastic deformation depends only on the stiffness of spring, which is selected by the user but not the real property of the material.

DDA was developed by Shi and Goodman[3] to analyze the stability of jointed rock originally. It solves block system where all the isolated blocks are taken as elements. The elements can be deformable and in any shape. All the blocks are connected together to a block system by penalty and shear spring set on contact and a kinematic equation is solved for dynamic and quasi-static problem. It can be used to calculate the deformation and stress distribution of block system at dynamic, quasi-static and static state. The advanced contact search method and contact and friction treatment makes this method can be used to simulate granular assembly like sand.

In this paper, we try to use DDA to simulate the stress and deformation of a sand model during cyclic loading. Some deformation properties of sand such as elasto-plastisity, dilatancy, strain softening, hysteresis loop during unloading-reloading can be clearly seen in the simulated stress-strain curve. By simulating the movement of particles and analyzing the force acted on them, the macroscopic behavior of the sand model is tried to be explained by the microscopic movement and stressing of particles.

2. DDA FUNDAMENTALS

DDA is used to deal with discontinuous material or block system. In DDA, every block is treated as one element. The elements or blocks used by DDA method can be of any convex or concave shape. When blocks are in contact, Coulomb's law is applied to the contact surfaces, and simultaneous equilibrium equations are selected and solved at each loading step or time increment. The large displacement (or movement of blocks) and deformation are the accumulation of small displacement and deformation at each time step. Within each time step, the displacement at all points are small, hence the displacement can be reasonably represented by first order approximation.

Assuming each block has constant stress and constant strain within small time step, the displacement (u,v) at any point (x,y) of block can be represented by six displacement variables:

$$\{D_i\} = \{u_0 \; v_0 \; r_0 \; \varepsilon_x \; \varepsilon_y \; \gamma_{xy}\}^T \qquad (1)$$

where $\{D_i\}$ is the unknown vector, u_0, v_0, r_0 the rigid body displacement at x,y direction and rotation, and $\varepsilon_x \varepsilon_y$ and γ_{xy} are the strains in the block.

As discribed by Shi et al.[2], the complete first order approximation of block displacement takes the following form:

$$\begin{Bmatrix} u \\ v \end{Bmatrix} = \begin{bmatrix} 1 & 0 & -(y-y_0) & (x-x_0) & 0 & (y-y_0)/2 \\ 0 & 1 & (x-x_0) & 0 & (y-y_0) & (x-x_0)/2 \end{bmatrix} \{D_i\} = [T_i]\{D_i\} \qquad (2)$$

where $[T_i]$ is the block deformation matrix.

Equation (2) expresses the relationship between deformation and block shapes, and block shape is updated by using equation (2) on each time step.

In the DDA method, individual blocks form a system through contacts of blocks and displacement constraints on single block. The simultaneous equilibrium equation of motion of dynamic problem is given as:

$$\left(\frac{2}{\Delta t^2}[M] + \frac{2}{\Delta t}[C] + [K]\right)\{\Delta D\} = \frac{2}{\Delta t}[M]\{\dot{D}\} + \{\Delta F\} \qquad (3)$$

where $[M]$ is the inertia matrix, $\{\Delta D\}$ is the increment of displacement, $[C]$ is the viscosity matrix, $[K]$ is the global stiffness matrix including stiffness of block, contact matrix and fixed point matrix. $\{\Delta F\}$ is the load vector increment including external forces, inertia forces, contact forces and friction vector. The details of equation (3) can be found in Shi's works[3]. In the calculation showed bellow, the static mode is used and the first and second terms in the left side of equation (3) are taken as zero.

In the discontinuous analysis, the contact problem between blocks should be treated with special attention. Contact of blocks makes the individual blocks into a system and ensures no penetration. In DDA, penalty method is employed to enforce contact restraints at block interfaces. As shown in Figure 1, when a point contacts with a line, a penalty in normal direction and a shear stiffness of shear component are added to the stiffness matrix. The value of shear stiffness depends on the friction condition. The criterion of friction conditions of a block surface follows Mohr-Coulomb's law expressed as following [4]:

$$\begin{aligned} &\tau_s < \sigma_n \tan\phi + c, \ \textit{shear stiffness} = K_s \\ &\tau_s >= \sigma_n \tan\phi + c, \ \textit{shear stiffness} = 0 \end{aligned} \quad (4)$$

By penalty and formula (4), the contact and friction at block surface can be simulated.

3. DEFORMATION PROPERTIES OF A SAND MODEL BY DDA

In order to capture the movement and stressing of every particle to investigate the mechanism of some specific characteristics of sand, a very simple model is used here. Sand particles are simplified as disks with 11 sides. The diameter of particles is 2.00mm. The specimen of 0.1m×0.193m formed by such kind of particles is shown in Figure 2. In the initial state, the first vertex of the particles is at the top and the line from the center to the first vertex of particles is vertically upward. The bottom of the specimen is fixed and its top is composed of a rigid plate where displacement-controlled loading can be placed. The two sides of the specimen are rigid plates on which lateral pressure can be added. In the calculation, static and plane strain mode is used. The elastic modulus is taken as E=1000MPa, Poisson's ratio is ν=0.25, self gravity is taken as zero and the friction angle between particles is $\varphi = 25°$ as used by Cundall[2]. The friction angle between particle and top, bottom and side plates are taken as 2°.

The penalty p_n and shear stiffness K_s are taken as the same for all the contacts. At the first step, an initial value is set as:

$$p_n = 100E_{\max}, \quad K_s = 0.4p_n \quad (5)$$

where: $E_{\max}$ is the maximum Yong's modulus

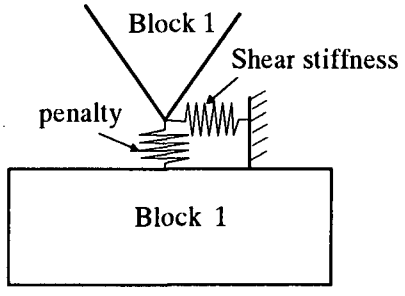

Figure 1 Contact mechanism

among all the block materials. And then they will be adjusted after a step calculation as bellow:

$$\begin{aligned} &p_n = \max\left(\frac{p_m}{0.0004}, 1/3\right)p_{n-1}, \\ &K_S = 0.4P_n \end{aligned} \quad (6)$$

where: p_m is the maximum penetration among all the contacts in *n-1* step calculation.

In the first stage of numerical calculation, consolidation pressure of $\sigma_1 = \sigma_3 = 200$kPa is loaded to make the intial state of shear loading and σ_3 is kept the same in all the calculation. After the consolidation, particles are in the most compact state with almost triangle layout. Then the displacement-controlled loading-unloading-reloading test is performed.

Figure 3 shows the deformation process of specimen and relative position of particles in some stages and Figure 4 shows the simulation results of shear stress $(\sigma_1 - \sigma_3)$-axial strain-volume strain relationship by DDA. Figure 5 gives the laboratory test result of stress-strain relationship of ChengDe sand (average grain diameter D_{50}=0.18mm, uniformity coefficient U_c=2.8, specific gravity of grain G_s=2.63, minimum void ratio $e_{\min}$=0.4, maximum void ratio $e_{\max}$=0.8, relative density D_r=0.64) under

consolidation stress $\sigma_3 = 100\,\text{kPa}$ and plane strain state. The internal friction angle of specimen obtained by DDA is 46°, which is slightly larger than the value of 41° by the laboratory test.

Comparing Figure 2 and 3 it can be seen that, although the shape, restriction and load are symmetrical in the initial state, but the deformed model is not symmetrical. The reason can be considered as the unsymmetrical deformation and motion of particles in microscopic view.

Comparison of Figure 4 and Figure 5 indicates that the stress-strain relationship by DDA shows the same pattern with that of the laboratory test. In the calculation result by DDA, most of the special deformation properties of sand such as elasto-plasticity, dilatancy, strain softening, hysteresis loop during unloading-reloading and volume contraction in unloading are well reproduced. The rotation and movement of each particle and their relating position change can be seen from Fig. 3. Consequently the phenomenon of macroscopic deformation of sand model can be related with microscopic motion of particles, to understand the microscopic deformation mechanism behind. Also the determination of qualitative relationship between microscopic motion of particles and macroscopic deformation of sand can be yielded.

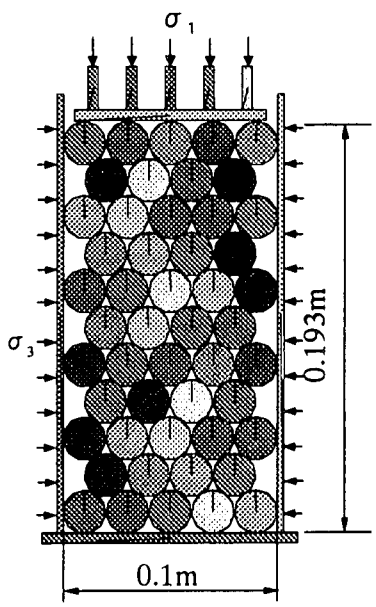

Figure 2. Configuration of the specimen in numerical test

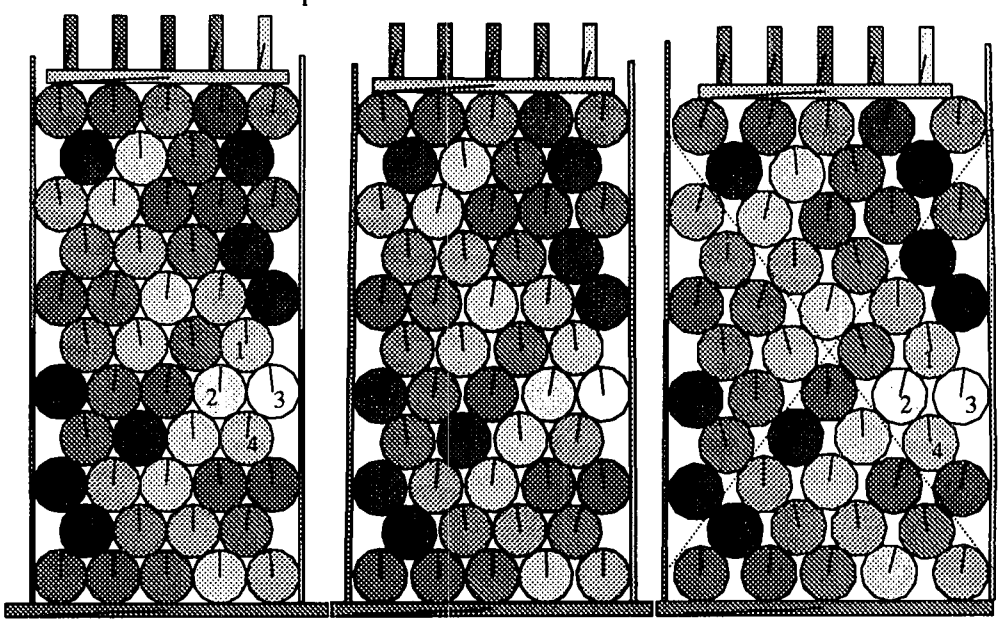

(a) After consolidation (b) Under peak load (c) In residual stress

Figure 3. Simulated process of partical motion

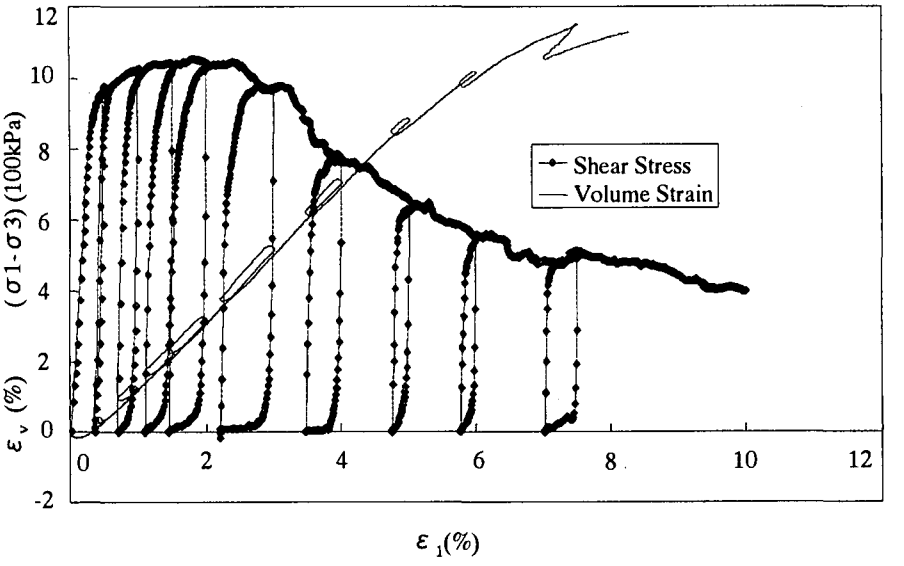

Figure 4. The calculated stress-strain curve by DDA (σ_3=200kPa)

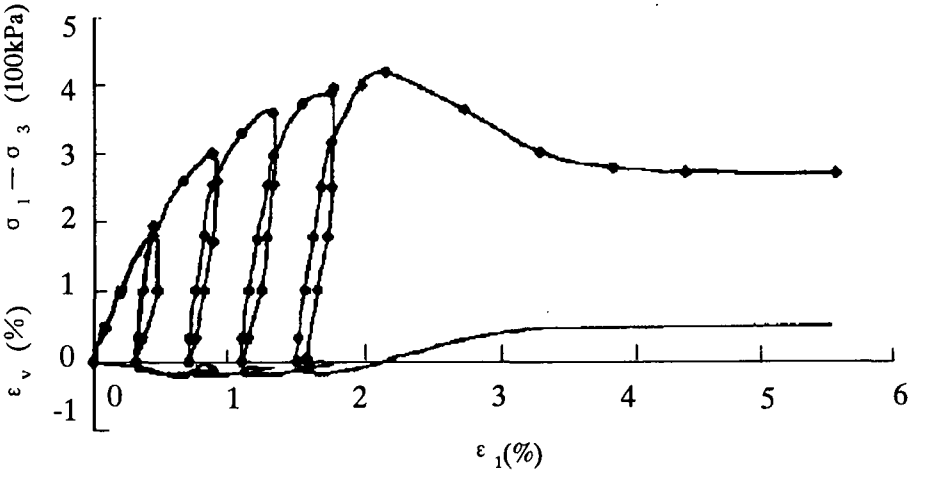

Figure 5. Laboratory test result of stress-strain curve for ChengDe sand (σ_3=100kPa)

4. MICROSCOPIC MECHANISM OF A SAND MODEL DEFORMATION

4.1 Elasto-plastic deformation

The total deformation of the specimen is composed of two parts, elastic deformation and plastic deformation. For sand like material, the elastic deformation is very small. Actually the elastic modulus of quartz-mineral materials is usually over than 10000 MPa. In the numerical calculation it is supposed that this value of particle is 1000 MPa. Although the calculated elastic deformation of particle is larger than that in the real situation, but it is only 0.1% from the consolidation state to peak load, is still very small compared with the plastic deformation. For the model in this paper, the plastic deformation of specimen is mainly caused by the relative movement of particles. As the function of friction between particles, the particles can not recover their placement even the shear stress ($\sigma_1 - \sigma_3$) is reduced to zero. Thus the unrecoverable plastic

deformation occurred. During unloading in Figure 4, when the shear stress $(\sigma_1 - \sigma_3)$ is larger than 200kPa, there is almost no relative movement between particles, the majority part of deformation belongs to elastic recovery. When unloading proceeded into its final stage, namely the shear stress $(\sigma_1 - \sigma_3)$ decreased to less than 200kPa, the plastic deformation occurred as resulting from the relative motion of particles, followed the formation of hysteresis loop. Comparing Figure 4 and Figure 5 it can be seen that, the computed stress-strain curve is similar to the experimental one.

4.2 Dilatancy

Dilatancy is a specific property of soil and sand in shear test. When consolidation is made, the specimen takes its mostly compacted state, and particles inside show a layout of triangle distribution {See Figure 6 (a)}. Under this condition the porosity of specimen is estimated as n=19% and minimum void ratio e_{min}=0.24. From Figure 5 it can be seen that, adding load up to the value of 80% peak load, particles start to move, leading to the decrease of density and the increase of porosity. It corresponds to the increase of specimen volume from the point of macroscopic view, at the same time it occurs the phenomenon of dilatancy. While at the state of residual strength, the particles of specimen take a layout of quadrate distribution and the specimen is most loosely composed. The porosity is approximated around n=38% and maximum void ratio e_{max}=0.46. In such case, the dilatancy can reach to ε_v =-19%. The calculated maximum dilatancy is only about ε_v =-12% due to the reason that friction exists at two ends of specimen.

4.3 Strain hardening with dilatancy

As a special deformation property of close sand, strain hardening happens with dilatancy. This phenomenon can also be seen from figure 4. At the beginning of loading, the volume strain decrease because the elastic deformation, but when the shear stress reaches to about 50 percent of the peak load, dilatancy begins to happen and the shear stress can still increase until the dilatancy reaches to about 2% (See Fig. 4). The reason of this phenomenon can be considered as bellow: when the shear stress reaches to certain level, some particles begin to move and some particles are pushed outward leading to the dilatancy, and then the stresses redistribute leading to a new steady state. The increasing of load is needed to cause new motion of particles till the shear zone is formed.

4.4 Strain softening

At compact state, particles of specimen take a layout of equilateral triangle distribution {Figure 6 (a)}. Angle of through central point lines is 60°. While at the residual strength state, particles of specimen changed to a layout of quadrate distribution. The angle of central point lines is 45° {Figure 6. (c)}. Static force analysis of particle 1 and 3 is made here to explain their force balance at peak strength and residual strength. Five forces acted on particle 3 are contact forces $P' = \dfrac{P_1}{2\cos\alpha(1+\tan\alpha\tan\phi)}$ with particle 1 and 4, friction forces $P'\tan\varphi$ with particle 1 and 4 and external force P_3. The balance analysis of particle 3 yields P_1=3.732 P_3 for compact state, which means particle 3 will start moving outward when P_1 equals 3.732P_3. In the numerical simulation, P_3 equals 200kPa. Acordingly from the balance analysis when P_1 equals 746kPa, plastic deformation of specimen will occur. The calculated force of P_1 is slightly larger than the analized value.

At residual strength state, static balance analysis to particle 3 yields P_1=1.732 P_3. It gives that the residual strength is about 46.6% of the peak strength. The result agrees well with the computation (Figure 4).

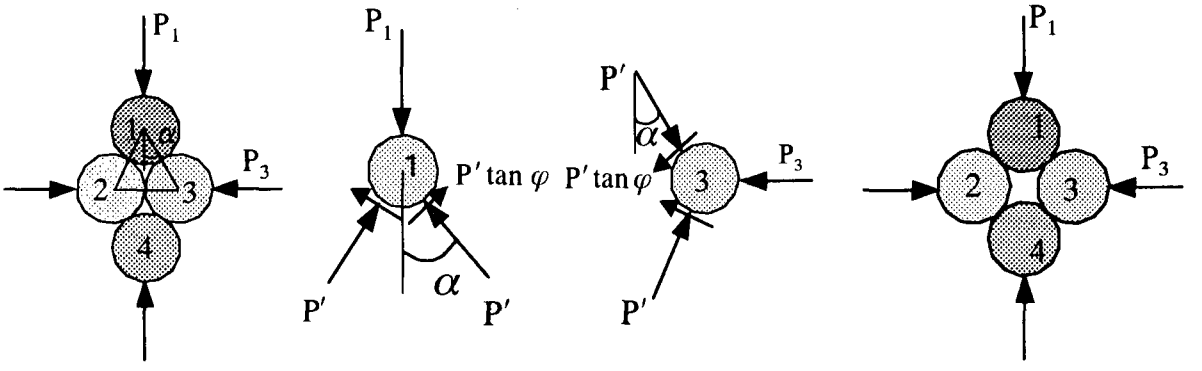

(a) Compact state (b) Forces acted on particle 1 and 3 (c) loose state

Figure 6. Sketch of the interaction between particles

4.5 Hysteresis loop during unloading-reloading

Both the laboratory test and numerical results illustrate obviously the hysteresis loop of stress-strain relationship as shown in Figure 4 and Figure 5. This phenomenon can be explained microscopically by the analysis of particle force balance or its movement. During loading process the particles start to move downward and outward corresponding macroscopically the vertical displacement and dilatancy of the specimen. While during unloading process, exist of friction makes the same particles unable to return to their original place even under the same stress with the loading process. At the beginning of unloading, particle 3 in Figure 6 stays unmoved with the decrease of P_1. Only when the decreasing of P_1 reaches to certain value at which P_3 becomes larger than the total horizontal components of force, particle 3 starts to move inward and particle 1 upward, macroscopically representing the upward displacement of the specimen. As reloading starts, P_1 is initially not large enough to push the particle to move. Only when the increasing of P_1 reaches to certain value that particles starts to move outward and downward, companied with the increase of plastic axial strain. For example, when $\alpha = 35°$, P_1 is required to be larger than $2.748P_3$ to push particle 3 moving outward during loading and reloading process. During unloading, however, particle 3 starts to move inward only when P_3 is larger than $1.192P_1$. It corresponds to the delay of sand deformation to the changing of load during unloading-reloading process that creates the formation of hysteresis loop.

4.6 Volume contraction in unloading

From the discussion above it is clear that, there is no movement of particles at the beginning of unloading. The deformation of specimen belongs to elastic recovery. Volume of specimen expands accordingly. As unloading proceeded, vertical load reduces and the horizontal load P_3 become large enough to push the particles moving inward and upward, leading to the recovery of a part of dilatancy, i.e. the volume contraction. This procedure is opposite with that of deformation during loading. Figure 4 shows that the loading part and unloading part at $\varepsilon_v - \varepsilon_1$ curve are nearly of parallel. This fact indicates that the volume contraction during unloading is the recovery of dilatancy during loading. On the other hand if unloading is made at the state when large deformation of specimen already obtained, the volume contraction becomes much more obvious compared with elastic recovery that the elastic recovery is too small to be observed in Figure 4. It was believed that sliding between particles belongs unrecoverable plastic deformation. The present study demonstrates that it is the recoverability of the inter-movement between particles that makes the dilatancy be recoverable.

Meanwhile during vertical compression test,

the layout of particles along vertical and horizontal directions shows different pattern (See Fig. 3(a)), that may be considered as anisotropy. Under hydrostatic pressure the horizontal force P_3 acted on particles is larger than the vertical one P_1, making the volume contraction starts from two sides of the specimen.
So that it can be say in some sense that the volume contraction is partly caused by anisotropy (Jiao and Chen[5]). Moreover, at triaxial test along some stress paths (for example $\sigma_1 + \sigma_3 = const$), the embedding of membrane caused by the increasing of σ_3 also increases the amount of volume contraction.

4.7 Formation of shear zone

Formation of shear zone can be seen in Figure 3 (c). When specimen enters into the state of residual strength, it becomes very loose, and a shear zone, which lies within the line of 52° to horizontal direction, formed {(See the dot line of Fig. 3 (c)}. This shear zone divided the specimen into two wedge parts. Direction of the shear zone is different from the theoretical value $(\frac{\pi}{4}+\frac{\varphi}{2})$. The reason is ascribed as that in the numerical simulation only few particles are used.

5. CONCLUSION

(1) This paper tries to use DDA to simulate the deformation of a sand model. By studying the movement, position and relationship of particles, together with the simulating result, same microscopic deformation mechanism of the sand model can be qualitatively explained.
(2) The deformation properties of sand as elasto-plastisity, dilatancy, strain softening, hysteresis loop during unloading-reloading, volume contraction during unloading and formation of shear zone are the result of movement of particles under different stress and restraint conditions.
(3) For sand, the relative movement of particles is not all unrecoverable. The recoverable dilatancy is the reason of volume contraction during unloading.
(4) For simplicity, a very simple model and some assumptions are taken in the present paper. In the further research, the influence of shape of particles and the parameters to the result should be studied and a model near to the actual sand should be used.

Acknowledgements: This study was jointly supported by the National Natural Science Foundation of China (No.559879008)

REFERENCE

1) P. W. Rowe: Theoretical meaning and observed values of deformation parameters for soil. Stress-strain behavior of soil (Ed. R. H. Parry). Roscoe memorial symposium. Cambridge University. 1972.
2) Cundall, P. A. And Strack, O.D.L.: A didiscrete numerical model for granular assemblies, Geotechnique, Vol. 29, No. 1, pp. 47-65, 1979.
3) Shi, G. H. and R.E. Goodman: Discontinuous deformation analysis. In C. H. Dowding &M. M. Sjngh (eds), Proc. 25th U. S. Symp. On Rock Mech. Evanston, AIME: 26-277,1984.
4) T. Sasaki, D. Ishii, Y. Ohnishi and R. Yoshinaka: Stability analysis of jointed rock foundation by discontinuous deformation analysis. Rock Foundation, Yoshinaka & Kikuchi (eds). Balkema, Rotterdam. Pp: 337-348,1995.
5) D. Q. Jiao and Y. J. Chen: The anisotropy of soil and the volume contraction in unloading. Journal of Rock Engineering (In Chinese). Vol. 16 (4), 9-15, 1994.

(Received April 21, 2000)